Analyst

Accepted Manuscript

This article can be cited before page numbers have been issued, to do this please use: X. Fan, Q. Yue, Y. Li, Y. Liu, L. Qu, Y. Cao and H. Li, *Analyst*, 2016, DOI: 10.1039/C5AN02543E.

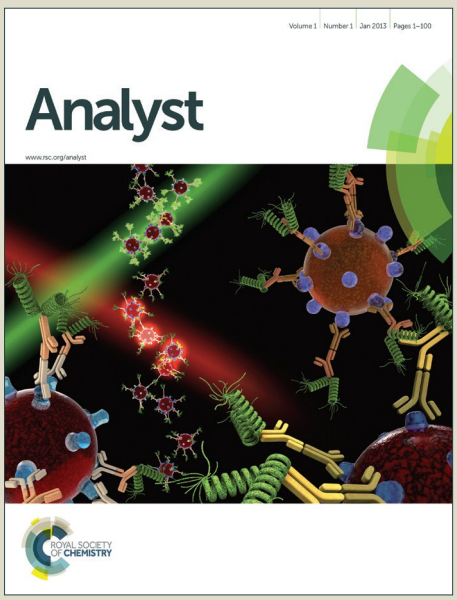

ROYAL SOCIETY OF CHEMISTRY

www.rsc.org/analyst

View Article Online
DOI: 10.1039/C5AN02543E

Analyst

ARTICLE

A single-bead telomere sensor based on fluorescence resonance energy transfer

Received 00th January 20xx,
Accepted 00th January 20xx

DOI: 10.1039/x0xx00000x

www.rsc.org/

Xiao Fan[a,#], Qiaoli Yue[b,#], Yanyan Li[a,#], Yingya Liu[a], Lu-Lu Qu[a], Yingnan Cao[a], and Haitao Li[a,c]*

We present a 200 nm in-diameter single-bead sensor for the detection of single, unlabeled DNA molecules in solution using fluorescence resonance energy transfer technology. DNA-bound Alexa 488 and Crimson 625 loaded on commercial beads served as the donor and acceptor, respectively. Binding of the target DNA to the single bead sensor induces G-quadruplex stretching, resulting in a decrease in fluorescence energy transfer. G-rich telomere sequences formed a G-quadruplex structure in the presence of ZnTCPP, as demonstrated by the detection of two strong donor and acceptor signals. The sensitivity of the sensor was 1 fM. Under optimized conditions using a polydimethylsiloxane microfluidic device, we measured the number of sensor beads by direct counting. By controlling the flow rate via the probe volume, one sensing experiment be can completed in 5 minutes. Based on these results, we propose a new parameter—dependability (Rs)—as a quantitative measure to judge the quality of a bio-sensor. This parameter is based on the ratio of sensor and sensing sample fluorescence signals. This parameter can range from 0.1 to 100, where a value of 10 represents an optimized bio-sensor.

Introduction

DNA sequences have important roles in molecular genetics.[1-4] Thus, much research has been devoted to developing a DNA sensor for enzyme detection in living cells. An ideal DNA sensor should exhibit high sensitivity and good selectivity. To accomplish this goal, various optical,[5, 6] electronic transduction,[7, 8] and surface plasmon resonance techniques have been employed. There are two assay formats used for DNA biosensors. The immobilization of enzymes,[9] antibodies,[10] or DNA probes[4] on a surface[11, 12] is commonly used in the development of enzyme electrodes, immunoassays, and DNA microarrays,[13] respectively, for use as DNA biosensors. Nonspecific interactions with the surface can be minimized by adding blocking agents, thereby optimizing performance.[14, 15] Another format is the homogeneous assay, in which the reactions take place in solution[16-18]. To amplify the signal in a homogeneous medium, several nanoparticle-based assays have been employed,[19] including silver-amplified scanometric detection,[20] silver-amplified electronic detection,[21] silver-amplified Raman fingerprinting,[22] magnetic microparticle-assisted DNA nanobarcode,[23] and conjugated polymer-amplified fluorometric assays.[24] More recent DNA detection approaches involve the use of fluorescent dyes, quantum dots, and nanoparticles. Methods using labeled nucleic acids coupled with quantum dots or nanoparticles offer high sensitivity of detection, but they suffer from several drawbacks that include particle aggregation,[25] toxicity,[26] and variation in the diameter of the nanoparticles.

Fluorescence resonance energy transfer (FRET) based on the non-radiative transfer of energy from a donor to an acceptor in close proximity (normally 1–10 nm) via long-range dipole-dipole interactions represents a typical homogeneous assay technique. In a FRET-based procedure, the donor and acceptor are brought into proximity for energy transfer exclusively as a result of the recognition of a target substance.[27] In addition to the high sensitivity afforded by a fluorescence assay, FRET techniques with advantage of low cost, convenient and simple to use are widely used to fabricate biosensors for detecting mycotoxins, H_2O_2, glucose and tumor marker.[28-32]

G-rich DNA sequences which can fold into noncanonical secondary structures (e.g., as in telomeric DNA) and spontaneously form four-stranded DNA structures called G-quadruplexes can be employed to build a FRET system.[33, 34] Intramolecular folding of a G-rich oligonucleotide into a G-quadruplex results in a compact structure stabilized by monocations[35] and ligands.[36] The folding/unfolding of specific G-quadruplex structures allows for the monitoring and detection of complementary target DNA sequences.[37-39] Combining the detection sensitivity of the single-molecule level and related

Contribution from the School of Chemistry and Chemical Engineering, Jiangsu Normal University, Xuzhou 221116, China
Department of Chemistry, Liaocheng University, Liaocheng 252059, China
Department of Chemistry, Cambridge University, Cambridge CB2 1EW, UK
#Equal contribution
**To whom correspondence should be addressed:*
Haitao Li
School of Chemistry and Chemical Engineering, Jiangsu Normal University, Xuzhou China
Tel, +8618905203826

View Article Online
DOI: 10.1039/C5AN02543E

techniques makes the telomere sequence well-suited for low concentration DNA analyses.[19] The length of a 21-bp duplex DNA is longer than that of a single-strand G-rich DNA molecule forming a G-quadruplex.[40] The formation of a G-quadruplex can be likened to the contracting movement of a piston in a cylinder, whereas a 21-bp double-stranded DNA molecule is like a rigid rod, with a persistence length of ≥100 bp.[41]

The dependence of FRET-based analyses on distance and orientation can provide valuable conformational information regarding G-rich nucleic acids. Quenching reagents such as tetramethylrhodamine[42] dye or gold nanoparticles[39] can be used to monitor the structure of a G-quadruplex, using fluorescein as a donor. In a recent study, gold nanoparticles were used as an acceptor in a FRET-based assay.[39]

In this study, we focused on developing a new biosensor, based on single-molecule fluorescence, to directly count the telomerase molecule and measure the structure at the same time, without sample separation and amplification. The method which is strongly dependent on donor - acceptor distance is label-free, low-cost, convenient and simple to use. We labeled fluorescent microspheres (F-microspheres) and a G-rich DNA with two dyes, Alexa 488 as the donor and Crimson 625 as the acceptor, with a G-rich DNA as a bridge. We then determined the fluorescence ratio in a FRET-based assay (Scheme 1). Single-stranded DNA labeled with an amino group (ssDNA) was first immobilized on F-microspheres via an amidation reaction. The F-microspheres were then modified with Alexa 488-labeled G-rich DNA by hybridization. In the presence of Zn(II)-5,10,15,20-tetrakis(4-carboxyphenyl)porphyrin (ZnTCPP), the G-rich DNA assumes a G-quadruplex conformation, resulting in FRET signal change and a subsequent increase in acceptor fluorescence intensity. However, upon the addition of target DNA, the G-quadruplex changes to a double-stranded helical structure, leading to weaker acceptor fluorescence signal. Compared with nanoparticles DNA sensors, this design will give clearly two separately donor and acceptor signals. In this way, we can avoid the effect of the wide distribution of nanoparticle fluorescence, which can decrease the FRET efficiency. This technique also has other advantages, as it is non-toxic and the brightness can be adjusted of the by changing the number of fluorescent molecules. Finally, a new theoretical method is proposed to rule out the dependability of a big and complicated biosensor, which at least contains four ssDNA, one dye molecule and onemicrosphere and easy-lost function during experiment.

Experimental

DNA constructs and reagents

All DNA samples (Table 1) used in this work were synthesized by Shanghai Sangon Biotechnology Co. and were purified by HPLC. All DNA samples were diluted with ultrapure water (Merck Millipore) after centrifugation at 6,800×g for 10 minutes. Fluorescent polystyrene microspheres (F-microspheres) loaded with crimson dyes (excitation and emission wavelengths of 625nm and 645 nm, respectively; Fig. 1) with carboxylate coupling surface were obtained from Life Technologies (Invitrogen). Protoporphyrin IX zinc (II) (ZnTCPP); >98%; Ekear) was used to stabilize G-quadruplex DNA. 2-Morpholinoethanesulfonic acid (MES; 99.5%) was purchased from Shanghai Shifeng Biological Technology Co. Tris-EDTA-NaCl (TEN: 5 mM Tris-HCl, 0.05 M NaCl, 1 mM EDTA, pH 6.0) buffer (10×) and N-(3-dimethylaminopropyl)-N-ethylcarbodiimidehydrochloride (EDAC, 98%) were obtained from Amresco, LLC. Potassium chloride (KCl, 98%), sodium chloride (NaCl), ethylenediaminetetraacetic acid (EDTA), Tween 20, and other common chemicals used in the study were obtained from Aladdin Industries (Shanghai) Co., LTD. Ultrapure water was obtained from a Milli-Q Reference water purification system (Merck Millipore). All reagents were used directly without any further treatment.

Characterization of oligonucleotides

Oligonucleotide absorption spectra were acquired using a NanoDrop 2000c spectrophotometer (Thermo Fisher Scientific). Fluorescence was measured using a NanoDrop 3300 fluorospectrometer (Thermo Fisher Scientific). A PHS-3C Delta 320 meter (Mettler Toledo, Switzerland) was used to measure pH. Desktop multifunction centrifugal ultrafilters were used (Eppendorf-5430).

Immobilization of DNA on fluorescent microsphere surfaces

To immobilize DNA on the surface of fluorescent microspheres, microspheres were first modified using probe 1 (NH_2-DNA, as shown in Table 1) based on amidation reactions involving the carboxyl groups on the microsphere surface and the amino group-labeled probe. First, 20 μL of fluorescent microspheres (2.3×10^{12}/mL) were diluted in MES (50 mM, pH 5.75) to 100 μL, and then the sample was centrifuged at 10,600×g for 10 minutes. The supernatant fraction was removed, and the resultant pellet was rinsed in MES buffer. Next, 35 μL of NH_2-DNA (100 μM) was added to the dispersed microspheres, followed by 4 μL of EDAC (10 mg/mL). The sample was incubated for 60 minutes with continuous shaking at 25℃. To enhance the amidation reaction, the final step (adding EDAC and subsequent incubation) was repeated 4 times. The desired product (F-microsphere/ssDNA) was collected by centrifugation at 10,600×g for 10 minutes and used for the subsequent measurement.

Hybridization

DNA hybridization was accomplished by a two-step procedure, as shown in Scheme 1. First, Alexa 488-labeled G-rich DNA (Alexa-GDNA) was hybridized with NH_2-DNA on the microspheres incubated in MES buffer for 8h at 25℃ to form F-microsphere/ssDNA/Alexa-GDNA. Second, the Alexa-GDNA was hybridized with the complementary target DNA. For the hybridization of Alexa-GDNA and ssDNA, F-microsphere/ssDNA and Alexa-GDNA were incubated in TEN buffer for about 12 hours to stabilize the base pairs in the absence of light. The resulting F-microsphere/ssDNA/Alexa-GDNA precipitate was collected by centrifugation, washed, and re-dispersed in MES buffer for subsequent fluorescence analysis. 18 μL ZnTCPP at 100 μM was added to the reaction mixture to drive formation of G-quadruplex DNA and stabilize the conformation. Target DNA (100 μM) (Table 1) with a sequence complementary to Alexa-GDNA was added after the folding of the G-rich single-stranded sequence into a G-quadruplex. A buffer pH of 5.75 was selected, and the ionic strength of the buffer was optimized to 1mM.[39] In

View Article Online
DOI: 10.1039/C5AN02543E

order to stabilize the sensor, the resulting solution was incubated overnight at room temperature in the dark, and then it was subjected to fluorescence analysis.

Single molecule fluorescence spectroscopy

The apparatus used for single-molecule FRET was similar to that described previously.[43-48] A 488-nm Gaussian beam (Spectra Physics Cyan CDRH) was directed through the back port of an inverted microscope (Nikon Eclipse Ti-U), where it was reflected by a dichroic mirror through an oil immersion objective (Apochromat 60×, NA 1.40, Nikon) and focused 5 μm into the microfluidic device. The focal spot was carefully manipulated to find the position of a single bead flowing through the microfluidic device.

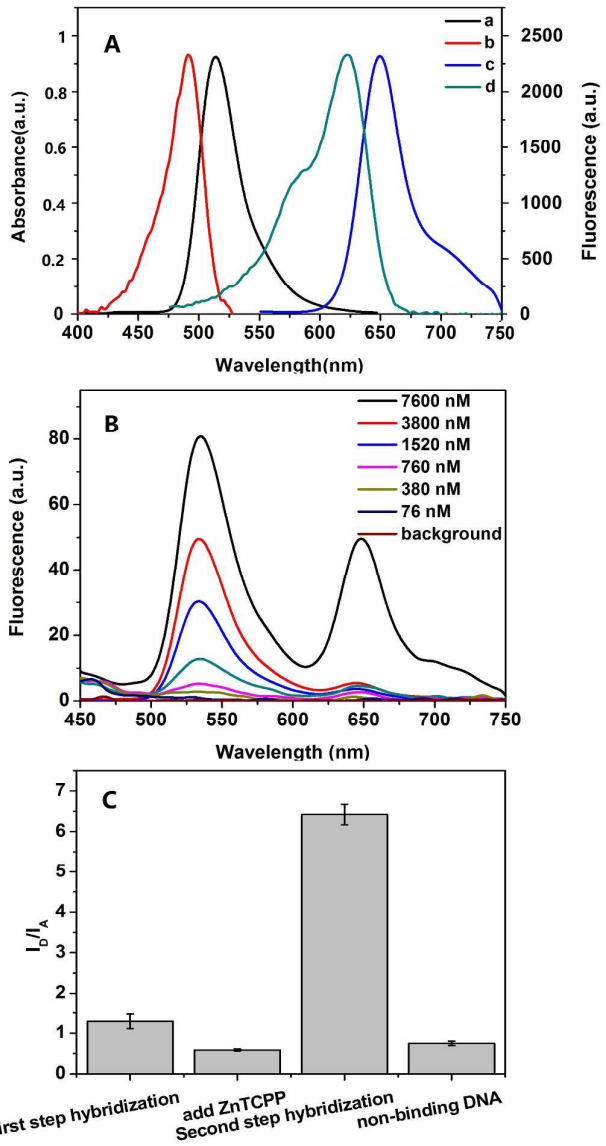

Fig. 1 Representative spectra detected by the DNA biosensor. a) Absorption spectra and fluorescence emission spectra of Crimson 625 and Alexa 488. Lines a and b represent fluorescence emission and absorption spectra of Alexa 488, respectively. Lines c and d represent fluorescence emission and absorption spectra of Crimson 625, respectively. b) Fluorescence spectra, and c) histogram of the F-microsphere/ssDNA/Alexa-GDNA system (sample III) under excitation at 450 nm. The sensor shows two well-separated peaks after the first hybridization step, shown by the black line. Adding ZnTCPP causes G-quadruplex conformation and induces a stronger acceptor signal, shown by the red line. With the addition of target DNA, the FRET signal weakened distinctly. In contrast, addition of non-binding ssDNA did not show obvious change of fluorescence spectrum.

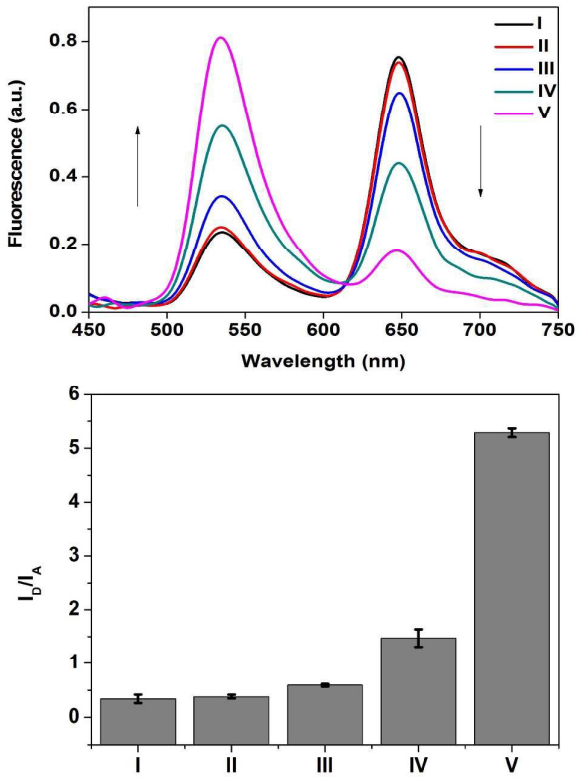

Fig.2 Fluorescence emission spectra of a single-bead sensor as afunction of increasing line DNA length. Line DNA, which established the distance between Alexa 488 and Crimson 625, varied in Samples I through V, ranging from about 3.82 nm (Sample I) to 10.62 nm (Sample V). As the length of single-stranded, line DNA increased, the FRET signal weakened.

Table 1 Oligonucleotide sequences used in the study

DNA sample	Sequence
I	5′-ATGCTCG X-3′
II	5′-ATGCTCGTTTTT X-3′
III	5′-ATGCTCGTTTTTTTTTT X-3′
IV	5′-ATGCTCGTTTTTTTTTTTTTT X-3′
V	5′-ATGCTCGTTTTTTTTTTTTTTTTTT X-3′
VI	5′-CGAGCATGGGTGGGAGGGTGGGAA Y-3′
VII (Target DNA)	5′-TTCCCACCCTCCCACCC-3′
VIII (Non-binding DNA)	5′-CCAAACTTACTTTCTAA-3′

Oligonucleotide sequences are modified with X, NH_2; Y, Alexa 488.

View Article Online
DOI: 10.1039/C5AN02543E

Fluorescence was directed through the same objective, imaged using a 100-µm pinhole (Melles Griot), and separated into two different channels using a dichroic mirror (585DRLP Omega Filters). Green fluorescence was filtered using long-pass and band-pass filters (540ALP and 535AF45, Omega Optical Filters) before being focused onto an avalanche photodiode (APD) (SPCM-14, Perkin Elmer). Red fluorescence was filtered using long-pass and band-pass filters (565ALP and 695AF55, Omega Optical Filters) before being focused onto a second APD (SPCM-14, Perkin Elmer). Dark count rates for the APDs were found less than 100 counts/s. Outputs from the APDs were coupled to two computer-integrated multichannel scalar cards (MCS-Plus, Perkin Elmer); the synchronous start output of one MCS-Plus card was used to trigger the second.

Microfluidic Device

The PDMS microfluidic device used in flow experiments was constructed as previously described. [43] The device dimensions were 100 µm (width) by 25 µm (height). Syringes (Hamilton, Gastight, 250 µL) were connected to the device via polyethylene tubing (Intramedic, internal diameter 0.38 mm). Flow was controlled using syringe infusion pumps (Harvard Apparatus PHD2000). The buffer and sample flow rates were identical. The flow rates indicated herein refer to the mean velocity calculated from the total flow rate and volumetric capacity of the microfluidic device.

Results and discussion

The FRET sensing mechanism

In Scheme 1, we diagram how changes in the FRET signal depend on the formation of G-quadruplex conformation. The signal is transferred between the donor- (Alexa 488) labeled 3' end of the G-rich DNA and the acceptor- (Crimson 625) loaded F-microsphere. The distance between the two fluorescent molecules is controlled by the folding of Alexa-GDNA into the G-quadruplex conformation, and by its subsequent stretching.

DNA samples (I-IV) were immobilized on F-microspheres based on an amidation reaction between the carboxyl groups on the microsphere surface and the amino group labels on the DNA molecule. Alexa 488-labeled G-rich DNA (sample VI) was hybridized with microsphere-attached NH_2-DNA, and then ZnTCPP was employed to drive conversion of the G-rich DNA into a G-quadruplex structure. After folding of the G-quadruplex, the distance between the donor and acceptor was shortened, resulting in FRET. As shown in Fig. 1B, the acceptor signal became stronger upon addition of ZnTCPP. After the target DNA with a sequence complementary to the Alexa-GDNA was added, the G-quadruplex unfolded and the Alexa-GDNA stretched. As the distance between the microsphere and the Alexa 488 dye molecule increased, the FRET signal decreased to undetectable levels, resulting in an obvious change in donor and acceptor signals (Fig. 1C). It is very hard to control the DNA conjugation and hybridization processes keeping the same quality of the sensor after multi-step operations. Before we start the formal experiment for data collection and analysis, we defined a new parameter, dependability (R_S) which is a key factor to describe the quality of the biosensor using a two-peak system as follows:

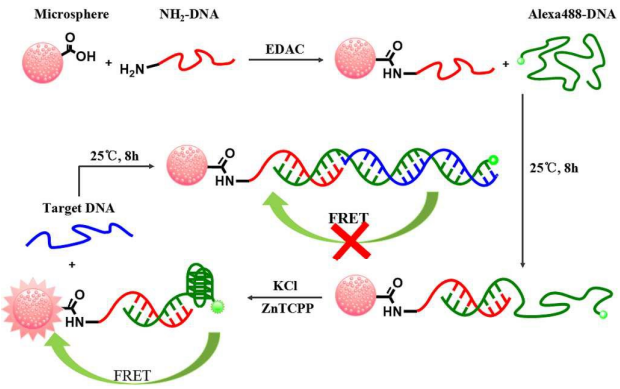

Scheme 1 Schematic construction of the single-bead sensor based on fluorescence resonance energy transfer (FRET). The F-microspheres (as acceptors) were conjugated with Alexa-DNA (the donor) in the presence of Zn(II)-5,10,15,20-tetrakis(4-carboxyphenyl)porphyrin (ZnTCPP), which induces G-rich DNA to change its conformation. The quadruplex structure forms in the presence of target DNA, leading to a decrease in fluorescence from the acceptor.

$$R_S = \frac{[I_D / I_A]_{Sample}}{[I_D / I_A]_{Sensor}} \quad (1),$$

where I_D and I_A are the intensities of the donor and the acceptor fluorescent peaks, respectively. $[I_D/I_A]$sensor is the FRET measurement of the sensor before reaction, and $[I_D/I_A]$sample is measurement of FRET after the sensor reacts with the sample. The ratio (R_S) indicates the dependability of the sensor, helping to prepare a standard curve of Rs with the length of DNA probe and quickly choose a sensor system with suitable quality for the target DNA sequence of interest. For example, fluorescence spectra acquired before and after stretching of the G-quadruplex are shown in Fig. 3. The length of random-coil double-stranded DNA ranged from 8.16 nm to 14.96 nm, and the FRET signal diminished as the length of the NH_2-DNA increased. The FRET signal for the F-microsphere/ssDNA/Alexa-GDNA system (defined as a single-bead sensor) (sample V) was undetectable. The R_S values for the single-bead sensors (samples I–V) were 13.39, 15.24, 9.66, 7.03, and 6.89, respectively (calculated the fluorescence peak height), or 14.97, 16.39, 10.88, 7.60, and 11.52, respectively (calculated the fluorescence peak area) (shown in Table S1 in the supplementary material).

If the donor and acceptor signal give similar fluorescence signals, e.g. single-bead sensors (sample III), the R_S value was around 10. This sensor was stable over the entire experimental period. For other samples (V and VI), the longer distance (>7.8 nm) between Alexa 488 and F-microsphere results in a weaker FRET signal and a R_S value <7. For sample I, the Alexa 488 and Crimson 625 fluorophores have less distance between them, making the RS value >15. In cases where the conjugated DNA on the bead tumbles to surface, [39] the shortest distance would be very close

View Article Online
DOI: 10.1039/C5AN02543E

to 0, and the resulting R_S value would be >100. These results suggest that this calculation could be used to gauge the dependability of the sensor. As a control experiment, non-binding DNA was added to the single bead sensor. The distance between donor and acceptor did not change in this case, resulting in an R_S value of approximately 1. If the DNA sequence is too long, no FRET signal will be produced, resulting in an R_S value <0.1.

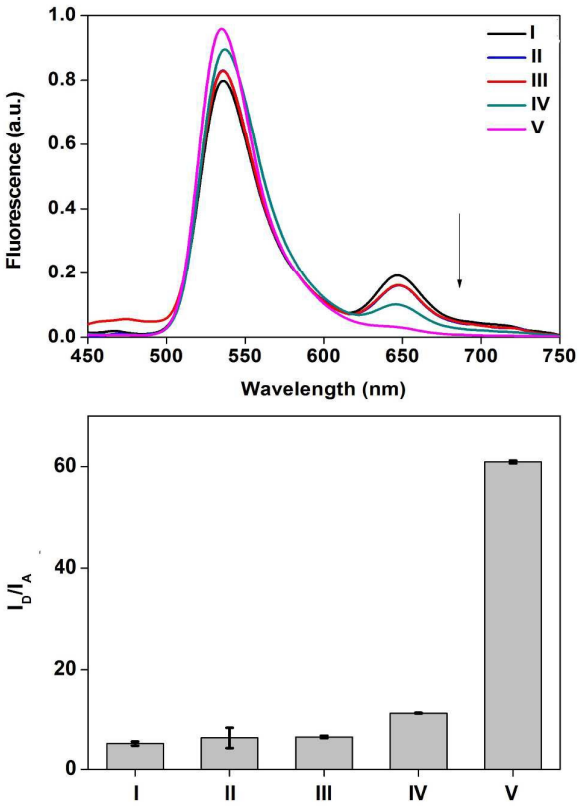

Fig. 3 Fluorescence emission spectra of a single-bead sensor with target DNA. With the addition of target DNA, the G-quadruplex structure stretched, causing the distance between the Alexa 488 fluorophore and the F-microsphere to range between 8.16 nm and 14.96 nm. As the length of ssDNA increased, the FRET signal weakened. The FRET signal from the F-microsphere/ssDNA/Alexa-GDNA system (sample V) became undetectable.

Effect of DNA length on FRET

FRET is significantly affected by the distance between the donor and the acceptor. Therefore, a series of NH_2-DNA sequences of differing length were introduced to study the effect on the FRET signal in the single-bead sensor system (Table 1). The number of bases in the NH_2-DNA sequences varied from 7 to 27, thus providing a range of distances between the donor and the acceptor.

Fig. 2 shows the fluorescence spectra acquired using the single-bead sensors varying NH_2-DNA length. The distance between neighboring bases is about 0.34 nm, thus the distances between the Alexa 488 and nearest surface of the bead after G-quadruplex formation in the 5 different sensors ranged from about 3.82 nm to 10.62 nm. The Alexa 488 fluorescence intensity increased and that of Crimson 625 decreased gradually with increasing NH_2-DNA length, suggesting that FRET diminished with greater NH_2-DNA length.

We also used molecular modeling to predict the possible distances between the fluorophore Alexa 488 and the surface of the bead (e.g., F-microsphere) and hence, determine the FRET efficiency for each case. Assuming a Förster distance, R_0, of 5.6 nm for Alexa 488/Crimson 625, we can estimate the contribution of the linkers to the interfluorophore distance as follows:

$$E = \frac{1}{1+\left(\frac{R+l}{R_0}\right)^6} \quad (2),$$

where R represents the distance between two labeling sites, as determined by modeling, and l represents the linkers' contribution to the distance. Both sets of linker-length contributions were evaluated. The length of C6 linker was 2.2 nm in this experiment. The distance between the Alexa 488 dye and the bead surface was corrected to 2.48–5.19 nm (Table 2).

The fluorescent spectra for samples I and II were similar because the fluorophore at the distal end can loop back and adsorb onto the same bead. Single-stranded DNA on the surface is flexible, a property that enables the adsorbed oligonucleotide to form an arch-like structure.[13, 23] Therefore, we chose to use sample III or sample IV for probe detection in subsequent experiments.

Effect of ZnTCPP on the system fluorescence

In the presence of monovalent cations (e.g., Na^+ or K^+), G-rich DNA sequences form a G-quadruplex that can inhibit telomerase activity, and thus inhibit the proliferation of cancer cells.[49, 50] G-quadruplex ligands, such as ZnTCPP, can stabilize the G-quadruplex formation. We used ZnTCPP to stabilize the folding of G-rich telomeric DNA sequences into G-quadruplexes.[39]

FRET measurements were conducted on the single-bead sensor in the presence and absence of ZnTCPP, shown in Fig. 1. Addition of ZnTCPP resulted in distinct quenching of the donor fluorescence with the sensor (sample III), indicating that the distance between the Alexa 488 and the bead surface was shortened and that the G-rich DNA sequence folded into a G-quadruplex when the ligand was added.

Single Molecule FRET Measurement in Flow

To characterize the limit of sensitivity of the telomere sensor, we conducted single-molecule FRET measurements using the single bead sensor. In this series of experiments, we diluted the single-bead sensor sample in buffer to picomolar concentration. A representative pair of FRET intensity burst trajectories observed with 5 pM of single-bead sensor is shown in Fig. 4. This experiment was carried out at a flow velocity of 2 cm•s^{-1}. Under these flow conditions, one bead typically spent 4 ms in the laser beam of the polydimethylsiloxane (PDMS) microfluidic device and provided clear donor and acceptor signals. When we increased the flow velocity to 20 cm•s^{-1} (data not shown), the signal to noise (S/N) ratio for the FRET measurements was still sufficient for data analysis. We also ran a control consisting of F-

View Article Online
DOI: 10.1039/C5AN02543E

microspheres alone, and no FRET was detected in the red channel. A further reduction in sample concentration to 5 fM still provided sufficient signal to complete the analysis in 5 minutes (data not shown).

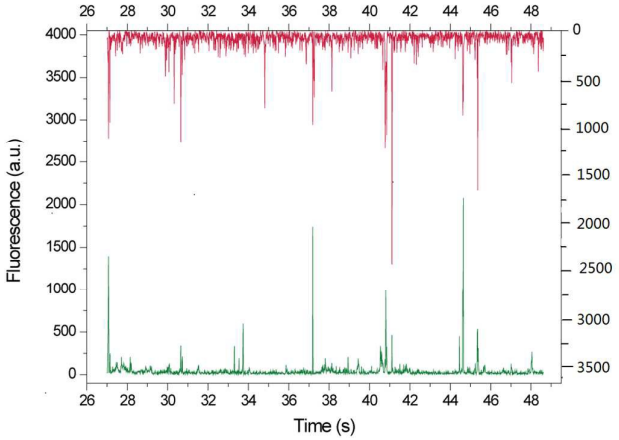

Fig. 4 Single-molecule FRET of single-bead sensor flowing through the microfluidic device. The blue trajectory represents the donor fluorescence signal and the red trajectory represents the acceptor signal.

Selectivity of the telomere sensor

We investigated the selectivity of the single-bead sensor for target DNAs by measuring the change in fluorescence after hybridization with single-base complementary (sample VII in Table 1) or non-binding (sample VIII in Table 1) single-stranded DNA. After the target DNA was added as illustrated in Fig. 1, the relative donor fluorescence intensity increased and that of the acceptor decreased, indicating that the G-quadruplex had stretched and the distance between the donor and acceptor had increased. As a control, we added non-binding DNA and observed no obvious change in fluorescence intensity, suggesting that the G-quadruplex remained stable. The data from this control experiment are provided in Table S1 and suggest the single-bead sensors should have good specificity for the target DNA in solution. This result demonstrates that the single-bead sensor is a useful and practical DNA sensor that can be used to detect specific target DNA.

Sensitivity of the telomere sensor

Using a direct imaging approach, Sauer et al.[51] combined the optimized parameters and enabled to achieve a detection sensitivity of ~ 10^{-11} M for realistic long fragmented DNA sequences in an overall assay time. Our previously described FRET system can be used for target DNA sensing at a detection limit as low as 40 pM.[39]

We investigated the applicability of the proposed FRET biosensor for quantitative sequence-specific detection of DNA. We systematically evaluated the signal amplifying property of our biosensor by hybridizing 9.47μM target DNA sequence (sample VII in Table 1) to the system at various concentrations. As shown in Fig. 5, the total fluorescence increased with increasing concentration of DNA. In contrast, and the microspheres linearly decreased with increased DNA concentration, suggesting that the experiment reached a limit at 100 nM in the buffer alone under the optimized condition.

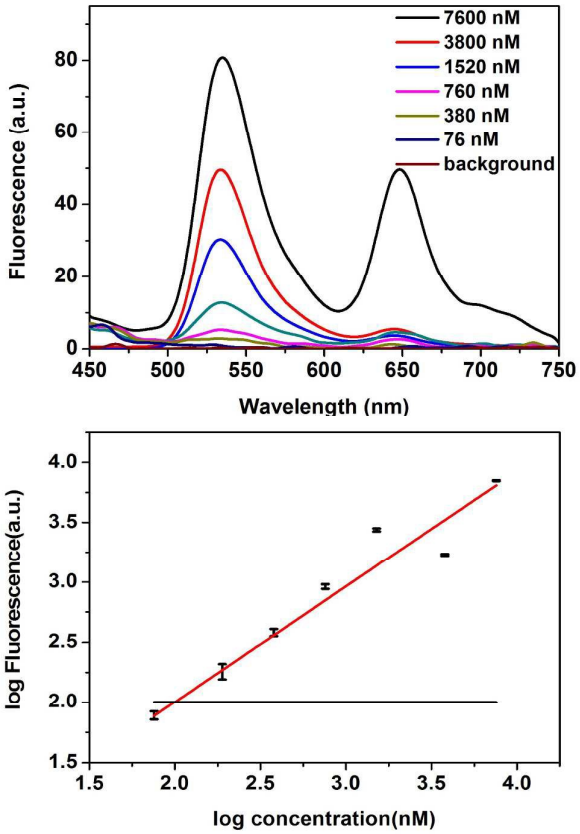

Fig. 5 FRET signal as a function of target DNA concentration. a) The fluorescence emission spectra, and b) the linear response of a single-bead sensor with the increasing concentrations of target DNA (0, 76 nM, 190 nM, 380 nM, 760 nM, 1520nM, 3800nM, and 7600nM). The error bars indicate the standard deviation of three separate measurements for each concentration of target DNA.

The density of carboxyl groups on the surface of the microspheres was 753 groups/bead,[52] whereas the local concentration of DNA on a single microsphere was 0.3 M and the concentration of microspheres in the modification step was 3.2×10^{-10} M. Therefore, the equilibrium constant (K) for ligand binding to the G-quadruplex DNA in solution was determined at $10^{5.54}$ using the following equation [53]:

$$K = \frac{[\text{complex}]}{[\text{sensor}][\text{target DNA}]} \quad (3)$$

Where [complex] represents the concentration of microspheres bound to the target DNA, [sensor] represents the concentration of local ssDNA/Alexa-GDNA system on a bead, and [target DNA] represents the concentration of free target DNA in solution. The target DNA limit of detection of the single-bead sensor was calculated at 3.08 fM, which matched the results of the single-molecule flow experiments.

View Article Online
DOI: 10.1039/C5AN02543E

Conclusions

In conclusion, we describe a 200-nm in-diameter, telomere sensor based on FRET which is non-radiative, convenient and simple, which can be used to perform ultrasensitive measurements of label-free DNA in solution. We have carried out both bulk and single molecule fluorescence experiments using this sensor. We introduce a parameter to describe the dependability of the sensor quality, which ranges from 0.1 to 100. Control of the flow of beads through the probe volume using a microfluidic device results in a substantial increase in the rate at which FRET events are detected, providing an experimental sensitivity 1 fM at a flow rate of 2 $cm \bullet s^{-1}$. Our results suggest a theoretical low limit of detection of 100 aM at higher flow rates, without adversely affecting the S/N ratio. This significant improvement allows for enhanced detection specificity and the characterization of DNA biosensors at fM-range concentrations.

Acknowledgements

This work was financially supported by awards from the Natural Science Foundation of China (21375051, 21505057 and 21005036), the Natural Science Foundation of Jiangsu Province (BK20150227), the Natural Science Foundation of Jiangsu Normal University (14XLR011), the Priority Academic Program Development of Jiangsu Higher Education Institutions, and the Brand Major of Universities in Jiangsu Province. This work was also supported by Natural Science Foundation of Shandong Province (2013SJGZ07 and ZR2014BQ017) and the doctoral research fund of Liaocheng University.

References

1X. J. Xie, W. Xu and X. G. Liu, *Acc. Chem. Res.*, 2012, **45**, 1511-1520.
2B. Liu, F. Liu, L. Fang, X. Wang and K. C. Chou, *Bioinformatics*, 2015, **31**, 1307-1309.
3C. Eckert, V. Gautier and G. Arlet, *The Journal of antimicrobial chemotherapy*, 2006, **57**, 14-23.
4L. Wang, E. Hua, M. Liang, C. Ma, Z. Liu, S. Sheng, M. Liu, G. Xie and W. Feng, *Biosensors & bioelectronics*, 2014, **51**, 201-207.
5G. D. Francia, V. L. Ferrara, S. Manzo and S. Chiavarini, *Biosensors & bioelectronics*, 2005, **21**, 661-665.
6S. Mariani, S. Scarano, J. Spadavecchia and M. Minunni, *Biosensors & bioelectronics*, 2015, **74**, 981-988.
7 M. Lin, Y. Wen, L. Li, H. Pei, G. Liu, H. Song, X. Zuo, C. Fan and Q. Huang, *Analytical chemistry*, 2014, **86**, 2285-2288.
8Z. G. Yu and R. Y. Lai, *Analytical chemistry*, 2013, **85**, 3340-3346.
9Y. Song, L. Wang, C. Ren, G. Zhu and Z. Li, *Sensors and Actuators B: Chemical*, 2006, **114**, 1001-1006.
10K. Omidfar, F. Khorsand and M. Darziani Azizi, *Biosensors & bioelectronics*, 2013, **43**, 336-347.
11M. F. Templin, D. Stoll, M. Schrenk, P. C. Traub, C. F. Vohringer and T. O. Joos, *Trends Biotechnol.*, 2002, **20**, 160-166.
12P. O. Brown and D. Botstein, *Nat. Genet.*, 1999, **21**, 33-37.
13T. H. Seefeld, A. R. Halpern and R. M. Corn, *Journal of the American Chemical Society*, 2012, **134**, 12358-12361.
14T. M. Herne and M. J. Tarlov, *J. Am. Chem. Soc.*, 1997, **119**, 8916-8920.
15E. R. Tovey and B. A. Baldo, *J. Biochem. Biophys. Methods*, 1989, **19**, 169-183.
16H. Zhang, F. Li, B. Dever, X.-F. Li and X. C. Le, *Chem. Rev.*, 2013, **113**, 2812-2841.
17A. A. Lubin and K. W. Plaxco, *Acc. Chem. Res.*, 2010, **43**, 496-505.
18D. Li, S. P. Song and C. H. Fan, *Acc. Chem. Res.*, 2010, **43**, 631-641.
19Y. Zhang, C. Pilapong, Y. Guo, Z. L. Ling, O. Cespedes, P. Quirke and D. J. Zhou, *Anal. Chem.*, 2013, **85**, 9238-9244.
20T. A. Taton, C. A. Mirkin and R. L. Letsinger, *Science*, 2000, **289**, 1757-1760.
21S. J. Park, T. A. Taton and C. A. Mirkin, *Science*, 2002, **295**, 1503-1506.
22Y. C. Cao, R. Jin and C. A. Mirkin, *Science*, 2002, **297**, 1536-1540.
23J. M. Nam, C. S. Thaxton and C. A. Mirkin, *Science*, 2003, **301**, 1884-1886.
24Y. Y. Wang and B. Liu, *Langmuir*, 2009, **25**, 12787-12793.
25H. Dong, W. Gao, F. Yan, H. Ji and H. Ju, *Analytical chemistry*, 2010, **82**, 5511-5517.
26A. Merkoci, *Biosensors & bioelectronics*, 2010, **26**, 1164-1177.
27K. E. Sapsford, L. Berti and I. L. Medintz, *Angew. Chem., Int. Ed.*, 2006, **45**, 4562-4588.
28J. C. Pickup, F. Hussain, N. D. Evans, O. J. Rolinski and D. J. S. Birch, *Biosens. Bioelectron.*, 2005, **20**, 2555-2565.
29S. Wang, N. Mamedova, N. A. Kotov, W. Chen and J. Studer, *Nano Lett.*, 2002, **2**, 817-822.
30 S. Wu, N. Duo, X. Ma, Y. Xia, H. Wang, Q. Zhang, *Anal. Chem.*, 2012, **84**, 6263-6270.
31 Q. Zhao, S. Chen, H. Huang, L. Zhang, L. Wang, F. Liu, J. Chen, Y. Zeng, P. Chu, *Analyst*, 2014, **139**, 1498-1503.
32 S. Ge, L. Ge, M.Yan, X. Song, J. Yu, S. Liu, *Biosensors & bioelectronics,* 2013, **43**, 425-431.
33D. Sen and W. Gilbert, *Nature*, 1988, **334**, 364-366.
34J. R. Williamson, M. K. Raghuraman and T. R. Cech, *Cell*, 1989, **59**, 871-880.
35Y. Wang and D. J. Patel, *Structure*, 1993, **1**, 263-282.
36N. W. Luedtke, *Chimia*, 2009, **63**, 134-139.
37.M. Deng, D. Zhang, Y. Zhou and X. Zhou, *Journal of the American Chemical Society*, 2008, **130**, 13095-13102.
38J. Ren, J. Wang, J. Wang, N. W. Luedtke and E. Wang, *Biosensors & bioelectronics*, 2012, **31**, 316-322.
39Q. Yue, T. Shen, C. Wang, L. Wang, H. Li, S. Xu, H. Wang and J. Liu, *Biosensors & bioelectronics*, 2013, **40**, 75-81.
40P. Alberti and J.-L. Mergny, *PNAS*, 2003, **100**, 1569-1573.
41G. S. Manning, *Biopolymers*, 1981, **20**, 1751-1755.
42J. L. Mergny and J. C. Maurizot, *Chembiochem*, 2001, **2**, 124-132.
43M. H. Horrocks, H. Li, J. U. Shim, R. T. Ranasinghe, R. W. Clarke, W. T. Huck, C. Abell and D. Klenerman, *Analytical chemistry*, 2012, **84**, 179-185.
44D. Alves, H. Li, R. Codrington, A. Orte, X. Ren, D. Klenerman and S. Balasubramanian, *Nature chemical biology*, 2008, **4**, 287-289.
45L. Ying, J. J. Green, H. Li, D. Klenerman and S. Balasubramanian, *Proceedings of the National Academy of Sciences of the United States of America*, 2003, **100**, 14629-14634.

View Article Online
DOI: 10.1039/C5AN02543E

46H. Li, X. Ren, L. Ying, S. Balasubramanian and D. Klenerman, *Proceedings of the National Academy of Sciences of the United States of America*, 2004, **101**, 14425-14430.
47J. D. Stephenson, H. Li, J. C. Kenyon, M. Symmons, D. Klenerman and A. M. Lever, *Structure*, 2013, **21**, 951-962.
48H. Li, D. Zhou, H. Browne and D. Klenerman, Journal of the American Chemical Society, 2006, 128, 5711-5717.
49A. M. Zahler, J. R. Williamson, T. R. Cech and D. M. Prescott, Nature, 1991, 350, 718-720.
50S. W. Liu, J. F. Chu, C. T. Tsai, H. C. Fang, T. C. Chang and H. W. Li, Analytical biochemistry, 2013, 436, 101-108.
51T. Klamp, M. Camps, B. Nieto, F. Guasch, R. T. Ranasinghe, J. Wiedemann, Z. Petrášek, P. Schwille, D. Klenerman and M. Sauer, *Sci. Rep.*, 2013, **3**.
52D. A. Thomson, K. Dimitrov and M. A. Cooper, *The Analyst*, 2011, **136**, 1599-1607.
53A. G. Kudrev, *Talanta*, 2013, **116**, 541-547.